

# Modeling of long-term creep behavior of structural epoxy adhesives

C.-W. Feng<sup>a</sup>, C.-W. Keong<sup>b</sup>, Y.-P. Hsueh<sup>b</sup>, Y.-Y. Wang<sup>c</sup>, H.-J. Sue<sup>a,\*</sup>

<sup>a</sup>Polymer Technology Center, Department of Mechanical Engineering, Texas A&M University, College Station, TX 77843-3123, USA

<sup>b</sup>Metal Industries Research & Development Centre, Kaoshong, Taiwan

<sup>c</sup>Dow Automotive, Auburn Hills, MI 48326, USA

Accepted 23 November 2004

Available online 1 April 2005

## Abstract

The mechanical properties of polymeric materials change over time, especially when they are subjected to long-term loading regimes. It is imperative that reliable accelerated tests be developed to determine the long-term time-dependent performance of polymers under different environmental conditions. The long-term creep behaviors of a neat epoxy resin and a commercial structural adhesive for bonding aluminum substrates were investigated. The time–temperature superposition method produced a master curve, allowing for the long-term creep compliance to be estimated. The physics-based coupling model was utilized and found to fit well with the long-term creep master curve. The equivalence of the temperature and moisture effects on the creep compliance of the epoxy adhesives was also addressed. Finally, a methodology for predicting the long-term creep behavior of epoxy adhesives was proposed.

© 2005 Elsevier Ltd. All rights reserved.

**Keywords:** A. Epoxy/epoxides; D. Creep; Coupling model; D. Viscoelastic

## 1. Introduction

Epoxy-based structural adhesives have emerged as a critical component for assembling structural parts due to their high strength-to-weight ratio, excellent adhesion properties, and superior thermal stability [1]. A structural adhesive can be defined as a load-bearing material with high modulus and strength that can transmit stress without loss of structural integrity. Compared with other joining methods, such as welding or bolting, epoxy-based structural adhesives provide exceptional advantages, including distributing stresses equally over a large area while minimizing stress concentrations, joining dissimilar materials, and reducing the overall weight and manufacturing costs.

However, epoxy resins, being viscoelastic in nature, exhibit unique time-dependent behaviors. This leads to a great concern in assessing their long-term load-bearing

performance, mainly because of a lack in fundamental knowledge of the viscoelastic behavior of epoxy-based structural adhesives. There is also a general concern regarding the lack of a long-term performance database for epoxy structural adhesives and the lack of a theory/model that can reliably predict the creep behavior of epoxy adhesives. Significant work is still required to develop accurate models for the prediction of the long-term behavior of epoxy adhesives, especially under different testing conditions.

Environmental exposure (moisture, UV, oxidation, etc.) during service is an important factor that needs to be considered when the long-term performance of structural adhesives is studied, since epoxy adhesives are expected not only to carry external loads but also to sustain thermal and/or moisture aging during service. It is crucial to understand how these environmental factors affect mechanical behavior. In this study, a neat epoxy resin (model system) and a commercial epoxy adhesive (commercial system) were chosen and exposed to various temperatures and environmental test conditions

\*Corresponding author. Tel.: 1 979 845 5024; fax: + 1 979 862 3989.  
E-mail address: hjsue@tamu.edu (H.J. Sue).

to determine how these factors influence durability and viscoelastic behavior. A viscoelastic model proposed by Ngai [2,3] was utilized to create a methodology for predicting the long-term creep behavior of epoxy adhesives under different environmental conditions, based on short-term experimental data in the linear viscoelastic range.

## 2. Theoretical consideration

The time–temperature superposition principle, which involves the reduced time concept, has been extensively utilized for estimating long-term performance of polymers [4–8]. Based on the assumption of thermorheological simplicity, short-term experimental data within the linear viscoelastic regime and at a reference temperature can be shifted individually to construct a master curve. The prediction of long-term creep responses at room temperature from deformation measured in accelerated tests at elevated temperatures can then be accommodated. The temperature dependence of the shift factors can be considered as an Arrhenius-type of behavior at temperatures below the glass transition temperature ( $T_g$ ) for amorphous as well as crosslinked polymers [9,10].

In the current literature, many empirical models have been applied to describe and predict the long-term viscoelastic behavior of polymeric materials. For example, the empirical power-law model seems to fit soundly, but only for short-term data [5,11], since the unlimited retardation spectrum from this model cannot describe the entanglement plateau region found in epoxy resins at longer times.

Another frequently utilized viscoelastic model is based on mechanical analogues of spring and dashpot elements [12]. Parallel and series combinations of these two basic elements have been found to fit experimental creep data adequately, even for complicated composite materials [13,14]. Generally, the more elements incorporated into the viscoelastic model, the more accurately the model can describe creep behavior. However, this type of viscoelastic model may not have direct physical significance in describing the viscoelastic behaviors of polymers.

The well-known Kohlrausch–Williams–Watts (KWW) equation [15,16], another commonly known model, has been shown to successfully describe the viscoelastic behavior of polymers by the use of a fractional exponential decay function [7,8]. However, the fractional exponential parameter that governs the breadth of the spectrum in the equation still lacks physical meaning, despite its ability to fit the experimental data quite well.

In present study, the coupling model introduced almost three decades ago by Ngai was used to analyze creep behavior in epoxy adhesives. An important

attribute of this model is its ability to physically describe the characteristics of the molecular mobility by means of a coupling parameter,  $n$ , and an apparent relaxation time constant,  $\tau^*$ . The coupling interaction between molecules and their surroundings is determined by  $n$  in a stretched exponential decay function. Based on this physical interpretation, the coupling model can be regarded as a predictive model since the  $n$  value can be predicted under different environmental conditions if the corresponding activation energies associated with molecular motions are known [17–19]. Another important characteristic of the coupling model is its ability to preserve the continuity from the primitive exponential function (Debye relaxation) smoothly to the empirical KWW function in an entire time-scale regime. The details of the coupling model can be found in Refs. [17–19].

With regard to material structural state, the coupling parameter reflects the degree of restriction on the molecular species to relax in a given environment [20]. An increase in intermolecular constraints associated with a higher crosslink density results in a larger  $n$  value [21]. Given the uniqueness of the physically based model, the coupling model can be regarded as a fundamental and intuitive model for describing the viscoelastic behaviors of polymers. For example, when the polymer absorbs moisture, one can easily predict (or expect) the  $n$  value to decrease due to the increased molecular mobility. The amount of reduction in  $n$  is related to the drop in activation energy due to moisture absorption. This unique capability makes the coupling model attractive. No other creep models in the literature, to our knowledge, offer such an apparent correlation.

Following the coupling model, the creep compliance can be described by the equation below:

$$D(t) = D_0 + (D_e - D_0)(1 - \exp[-(t/\tau^*)^{1-n}]), \quad (1)$$

where  $D(t)$  is the creep compliance as a function of time and  $D_0$  and  $D_e$  are the initial and equilibrium compliances, respectively.

Here, the details of how to derive the two crucial parameters,  $D_0$  and  $D_e$ , are addressed. In the linearly viscoelastic region, the creep compliance,  $D(t)$ , primarily depends on time ( $t$ ) and temperature ( $T$ ) in the form

$$D(t) = \frac{\varepsilon(t, T)}{\sigma_0}, \quad (2)$$

where  $\varepsilon(t, T)$  is the strain as a function of time and temperature and  $\sigma_0$  is the initial stress.

Based on the relationship derived from the Boltzmann Superposition Principle, [2] the initial compliance,  $D_0$ , can be estimated as

$$D_0 = \frac{1}{E_0}, \quad (3)$$

where  $E_0$  is the modulus as  $t \rightarrow 0$ .  $E_0$  can also be equated to Young's modulus obtained from a constant strain-rate tensile test. The value of shear modulus,  $G$ , from the dynamic mechanical test result can be represented by storage modulus,  $G'$ , and loss modulus,  $G''$ , in complex form

$$G = G' + iG'' \quad (4)$$

In the rubbery plateau stage, at which the ratio of loss and storage modulus is approximately 2–4%, the loss modulus can be neglected, and the complex modulus is equivalent to the storage modulus. Hence the equilibrium modulus can be derived from the rubber plateau modulus,  $G_r$  [22]:

$$E_e = G_r 2(1 + \nu), \quad (5)$$

where  $\nu$  is Poisson's ratio.

As for the equilibrium compliance,  $D_e$ :

$$D_e = \frac{1}{E_e}, \quad (6)$$

where  $E_e$  is found via Eq. (5) with  $\nu = 0.5$ , since the epoxy resin material is in the rubbery state. The relationships shown in Eqs. (3) and (6) were shown valid only for viscoelastic materials as  $t$  approaches zero or infinity [23].

Few studies that address the viscoelastic behaviors of polymers with combined moisture and loading effects can be found because the coupled effects give rise to complex viscoelastic properties. Modeling of effects of moisture on the mechanical behavior of polymers remains an open concern, even when the hydrothermal exposure is only restricted to physical interactions. Time–humidity superposition has been proposed to predict long-term performance of polymers using several short-term creep data at different relative humidities [24]. Nevertheless, arbitrary correction factors are required to generate a smooth master curve and compensate for the non-linear portion of the creep response. Wang et al. [25], however, found that the time–temperature–moisture superposition may not be applicable to construct the master curve of glass bead–epoxy composites.

Other studies focus on the creep behavior of polymers that have already possessed a certain level of moisture. An attempt was made to quantitatively establish the equivalence between temperature and the presence of moisture on the creep behavior of epoxy composites [5]. Unfortunately, the loss of the water from the wet plain matrix during the tests (especially at elevated temperature) was reported in both cases [6,25], which resulted in an inability to construct master curves.

In this study, the viscoelastic behaviors of epoxy adhesives under a dry condition and under the collective effects of exposure to a humid environment are

described with the use of Ngai's coupling model. The effectiveness and limitations of this model for predicting the long-term creep behavior of epoxy adhesives in humid environments is also discussed.

### 3. Experimental

#### 3.1. Material

Two sets of epoxy systems were chosen for this study: a model and a commercial epoxy adhesive system. Material details are given in Table 1.

The model epoxy system is composed of diglycidyl ether of bisphenol A (DGEBA) epoxy and a polyamide curing agent mixed at a stoichiometric ratio, along with a high-molecular-weight flexibilizer, i.e., DER 732, at 5% equivalent weight, to increase its flexibility. The commercial epoxy system is a two-component adhesive system with a high percentage of loading of hollow glass beads, which are widely used in controlling the adhesive thickness for structural applications.

The model system has a base formulation of the commercial epoxy adhesive system, which can be considered as a reference epoxy to help gain fundamental knowledge on the creep behavior of epoxy adhesives. The curing schedule for each system was 50 °C for 1 h and 120 °C for 3 h, followed by cooling in an oven overnight. The curing schedule to reach the fully cured state was determined on a differential scanning calorimeter (DSC) in isothermal tests (Perkin-Elmer Pyris-1). The attenuated-total-reflectance FTIR (ATR-FTIR) spectroscopy analysis was performed on a Nicolet AVATAR 360 system. Results showed the absence of a peak at 910 cm<sup>-1</sup> (epoxide groups), confirming that a fully cured epoxy network structure was attained. The cured resins were put in a vacuum desiccator for a minimum of 3 days. Annealing of each specimen at its respective  $T_g + 10$  °C for 30 min was performed to help remove any possible thermal history.

Table 1  
Material list of the model and commercial epoxy resin systems

Model epoxy resin system	
DER <sup>®</sup> 331	Dow Chemical; <i>EEW</i> <sup>a</sup> : 182–192
DER <sup>®</sup> 732	Dow Chemical; <i>EEW</i> <sup>a</sup> : 305–335
Versamid <sup>®</sup> 140	Cognis Corporation; <i>HEW</i> <sup>b</sup> : 97
Commercial product system	
BETAMATE <sup>™</sup> 73316/73317	Dow automotive

<sup>a</sup>Epoxide equivalent weight.

<sup>b</sup>Hydrogen equivalent weight.

### 3.2. DMA tests

DMA tests were performed in torsional mode on a Rheometrics RMS-800 with 5 °C per step at a frequency of 1 Hz. Strain sweep tests were first conducted at a strain range of 0.01–0.5% to determine the linear viscoelastic range. A 0.1% and a 0.15% sinusoidal strain were chosen for model and commercial system, respectively, to keep the tests within the linear viscoelastic region and to give a high signal-to-noise ratio.

The samples were tested at temperatures ranging from –90 to 160 °C. The transition temperatures, at the highest localized tangent delta peak values ( $\tan(\delta)$ ), were assigned as  $\alpha$ -transition ( $T_g$ ) and  $\beta$ -transition ( $T_\beta$ ) temperatures. The temperature sweep tests at frequencies of 0.1, 1.0, and 10 Hz were conducted to determine the degree of shift in tangent delta peak as a function of frequency.

### 3.3. Tensile tests

The tensile tests were conducted in accordance to ASTM Standard D638 (Specimen Type IV) on a Sintech-II Mechanical Test System. The engineering moduli were investigated at different temperatures under both dry and moisture saturated conditions. Tensile tests were performed at a crosshead speed of 2"/min, and axial strains were recorded with an extensometer attached to gage section of the samples.

Specimen temperature was controlled in an environmental chamber using a heater and an OMEGA CN76000 temperature controller linked with a thermocouple located at about 2 mm from the sample. Care was taken for tests performed at elevated temperatures. The Young's modulus was determined from the initial slope of the stress-strain curve. Good linearity of the stress-strain curves was observed for all samples tested up to 67 °C.

### 3.4. Moisture absorption tests

The model and commercial epoxy systems were first exposed to an environment of 95% relative humidity (RH) at different temperatures and were monitored frequently over a 5-month period. Moisture uptake data were then fitted by means of an equation based on Fick's law of diffusion [26], and the moisture saturation levels were noted by frequent weighing samples. To accelerate the moisture uptake, dry specimens were submerged in deionized water to help them reach their saturation level more rapidly. ATR-FTIR spectroscopy analysis was utilized on both systems during the immersion experiments to ensure that no unexpected chemical reactions occurred. When the submerged samples reached the same level of moisture uptake as those saturated samples exposed to 95% RH, the samples were placed

in a 95% RH environmental chamber for 24 h to guarantee that the samples remained saturated until testing.

### 3.5. Creep tests

A custom-built creep station, shown in Fig. 1(a), was used to carry out the creep tests. A constant load was applied to the specimens by means of a pneumatic cylinder (Motion Controls, D series), and a constant temperature was maintained inside the environmental chamber with a temperature controller (OMEGA CN76000). The vertical displacement, which was measured with an LVDT sensor (Solartron Mach1 series;  $10^{-3}$  in resolution), and the corresponding time were automatically recorded using LabView<sup>®</sup> software.

The dimensions of the creep test specimens were 100 mm × 15 mm × 1.5 mm, as shown in Fig. 1(b). A hole was drilled at each end of the sample and a spacer was attached to prevent slippage near the grip region of the specimen. The gage length was defined as the distance between the two spacers for each sample. The slippage and local stress concentration near the grip were minimized via the spacers and pins of the clamps, respectively. Since the spacer is relatively soft, it carries minimal load distribution during the creep test. It does not affect the creep test results.

The specimens were tested at different temperatures under dry (dry condition) and 95% RH (wet condition) environments. The determination of the stress level in the linear viscoelastic region was made by conducting a series of isochronous creep tests at the lowest and the highest test temperatures. The applied load was chosen to generate a 0.3% strain for each system. Each test was performed for 30 min to achieve an equilibrium environmental condition before each 1-day creep experiment. At least three creep tests were performed for each condition to ensure reproducibility.

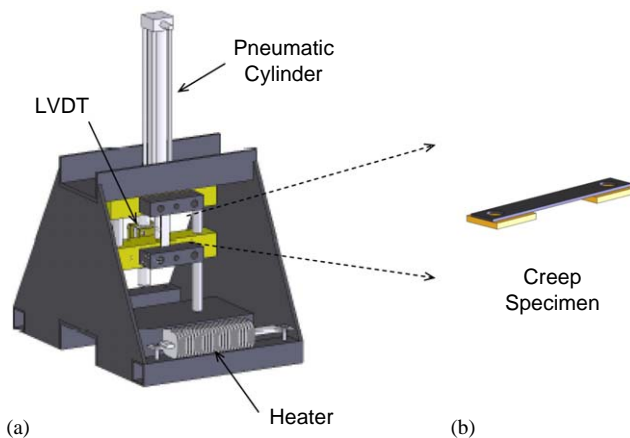


Fig. 1. The illustrations of (a) the creep station, and (b) the creep specimen.

In performing the time–temperature superposition creep tests, it was found that 67 °C was the highest temperature from which good time–temperature superposition of the short-time creep curves into a long-term creep master curve could still be achieved. This implies that the linear viscoelastic behavior of the epoxy samples has been maintained at least up to 67 °C.

**4. Results**

**4.1. Tensile tests**

Tensile moduli, as a function of temperature, for each system are shown in Fig. 2. The arrows indicate the moduli at the temperature where their values drop to 50% of the room temperature values. Those temperatures were chosen as the highest for creep testing for each epoxy system in the dry condition. As shown in Fig. 2, it is evident that the test temperature has a significant effect on the modulus of the epoxy systems, especially for the commercial epoxy system, which has a rather low  $T_g$ .

**4.2. DMA tests**

The model and commercial epoxy systems reach their moisture saturation content at 4.0% and 3.0% by weight gain, respectively, after the water immersion test.

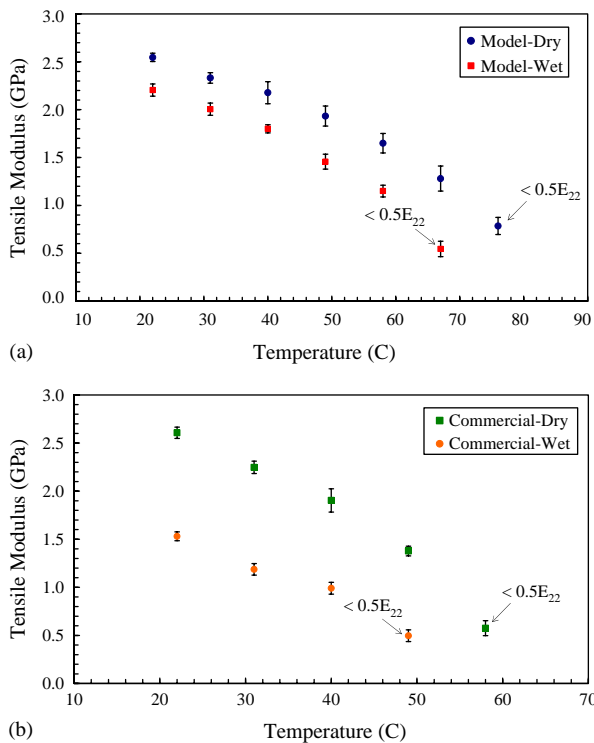


Fig. 2. The tensile moduli of (a) model epoxy system and (b) commercial epoxy system as a function of temperature.

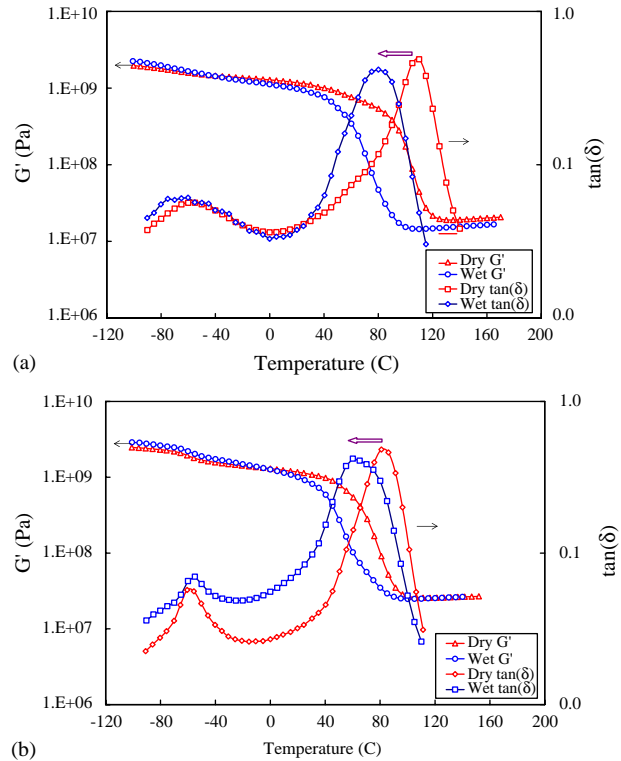


Fig. 3. DMA results (a) model and (b) commercial systems under different environmental conditions.

The drops of  $T_g$  for both systems, shown in Fig. 3, were determined with DMA tests at 1 Hz. The  $T_g$  drop due to moisture absorption follows the Fox equation [27]

$$\frac{1}{T_g^f} = \frac{W_m}{T_g^m} + \frac{W_w}{T_g^w}, \tag{7}$$

where  $T_g^f$  is the final-state glass transition temperature,  $T_g^m$  and  $T_g^w$  (−150 °C) are the glass transition temperatures of the polymer matrix and water, and  $W_m$  and  $W_w$  are the weight fractions of the matrix and water. The temperature takes an absolute temperature unit in this relationship. The comparisons between those  $T_g$ s obtained by the DMA tests and those derived from the Fox Eq. (5) are listed in Table 2.

The frequency sweep tests of the model system at 0.1, 1.0 and 10 Hz show the frequency dependence of  $T_\beta$  (Fig. 4). The  $T_\beta$  transition reflects the molecular mechanisms responsible for the creep process at a higher temperature, i.e., room temperature. The activation energy values for each transition can be obtained by an Arrhenius type of relationship between frequency,  $f$ , and  $T_\beta$ , as follows:

$$f = C_\beta \exp\left(\frac{E_\beta}{RT_\beta}\right), \tag{8}$$

where  $C_\beta$  is a frequency constant,  $E_\beta$  is the activation energy, and  $R$  is the Boltzmann constant. Fig. 5 shows an example of the Arrhenius relationship between  $\log(f)$

Table 2  
Comparisons of  $T_g$  before and after water immersion test

System	Glass transition temperature $T_g$ (°C)		
	Dry	Wet	Estimated by Fox Equation
Model	110	80	80
Commercial	80	60	61

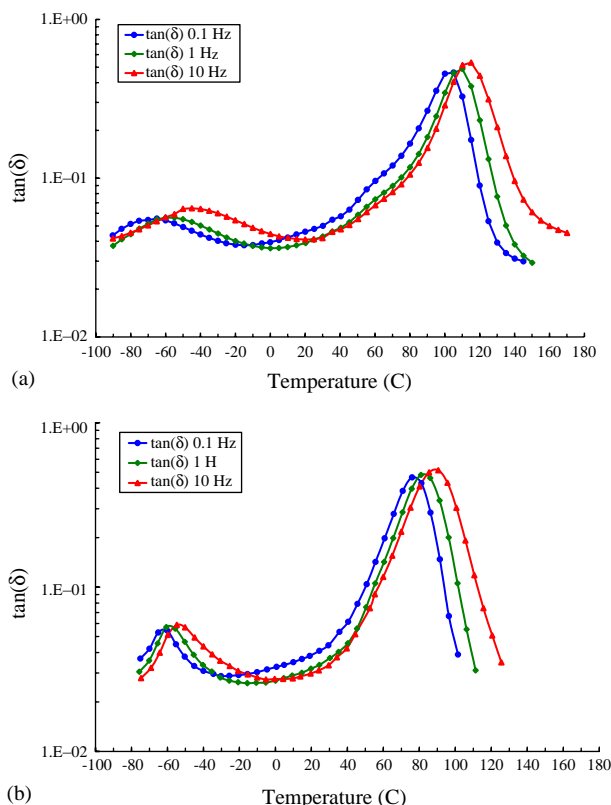


Fig. 4. DMA  $\tan(\delta)$  of (a) model system and (b) commercial system in dry condition operated at frequencies of 0.1, 1.0 and 10 Hz.

and  $1/T_\beta$  in the dry condition. Table 3 shows the complete list of  $T_\beta$ s at different frequencies and the activation energies of both epoxy systems.

4.3. Creep tests

Fig. 6 shows the creep compliance of the model epoxy system and the master curve at 22 °C as superimposed by each short-time creep compliance curve at a different temperature. The coupling model was applied to curve fit the master curves of each system (shown in Figs. 6(b)–8). In Fig. 9, the shift factors below  $T_g$  were plotted as a function of  $1/T$ , in accordance with the Arrhenius equation

$$A = A_0 \exp\left(\frac{E_a}{RT}\right), \tag{9}$$

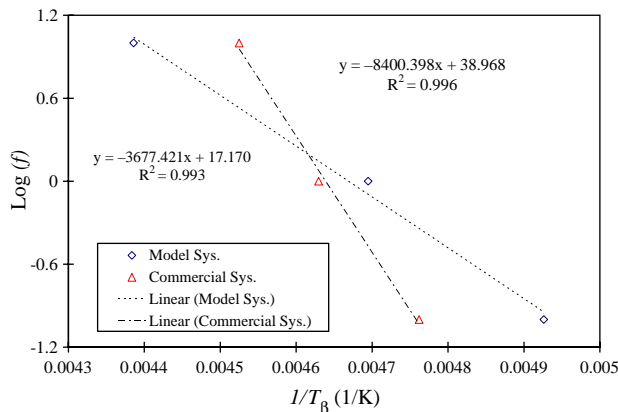


Fig. 5. The Arrhenius relationship between beta transition temperature and frequency in the dry condition.

where  $A$  is the shift factor,  $A_0$  is a constant,  $E_a$  is the apparent activation energy,  $T$  is a testing temperature in °K, and  $R$  is Boltzmanns constant.

Table 4 shows the parameters of the coupling model for each master curve. The creep behavior of the commercial epoxy system in the wet condition is not reported due to its non-linear viscoelastic responses even at relatively low temperatures (e.g., 30 °C). As a result, the creep compliance curve of the commercial epoxy system under the wet condition could not be shifted to form a smooth master curve.

When individual isochronous creep curves were compared under different conditions, it was found that the model epoxy system had a similar viscoelastic response when at a higher temperature in the dry condition and at a lower temperature with saturated moisture content (Fig. 10). Fig. 10(a) shows the equivalence between the dry creep compliance at 62 °C and the wet creep compliance at 40 °C (Case I). Similarly, Fig. 10(b) shows the equivalence between the dry compliance at 51 °C and the wet compliance at 31 °C (Case II). Following the Arrhenius relationship (Eq. (9)), the dry creep curve at 62 and 51 °C have been shifted 1.5 and 2.0 from those at 58 and 49 °C, respectively. Both cases show that each group of creep curves match well, suggesting that the presence of absorbed moisture can bring about the same creep response in the dry condition, but at a higher temperature.

Table 3  
Beta transition temperatures

System	Beta Transition Temperature $T_\beta$ ( $^{\circ}\text{C}$ )			$E_\beta$ (kJ/mol)
	0.1 Hz	1 Hz	10 Hz	
<i>(a) In the dry condition at different frequencies</i>				
Model	–70	–60	–45	70
Commercial	–63	–58	–53	180
<i>(b) In the wet condition at different frequencies</i>				
Model	–75	–65	–50	67
Commercial	–60	–55	–50	180

Table 4  
Parameters for the coupling model to fit the master curves

System	$D_0$ ( $10^{-8} \text{ Pa}^{-1}$ )	$D_c$ ( $10^{-8} \text{ Pa}^{-1}$ )	$\tau^*$ (s)	$n$
Model-dry	0.04	1.75	$1.4 \times 10^9$	0.73
Model-wet	0.05	2.30	$4.7 \times 10^6$	0.51
Com.-dry	0.04	2.20	$1.4 \times 10^7$	0.60

Table 5  
The equivalence of temperature and moisture effect on creep behaviors and the moisture effect on  $T_g$

	Temperature (dry vs. wet)		$T(\text{K})/T_g(\text{K})$	
	Case I	Case II	Case I	Case II
Dry	62 $^{\circ}\text{C}$	51 $^{\circ}\text{C}$	0.88	0.85
Wet	40 $^{\circ}\text{C}$	31 $^{\circ}\text{C}$	0.89	0.86

## 5. Discussion

The tensile test results indicate that the mechanical properties deteriorate severely when the testing temperatures are increased (Fig. 2). The moduli of model and commercial epoxy systems in the wet condition were reduced by 20% and 40%, respectively, suggesting the moisture exposure indeed affects the mechanical performance significantly even with only a small amount of moisture uptake. From the DMA results (shown in Fig. 3), the broadening of the  $\tan \delta$  peaks also suggests that moisture acts as a plasticizer in the epoxy matrix.

The loss of absorbed water may affect the  $T_g$  results from DMA, resulting in a misleading value compared with the theoretical  $T_g$  calculated from the Fox equation in the wet condition. A deviation of 15  $^{\circ}\text{C}$  between experimental and theoretical values has been shown [25]. However, from Table 5, the good agreement between the theoretical and experimental data by using our water immersion method shows that the Fox equation is applicable for the prediction of  $T_g$  drop with the presence of water in the matrix, and there is a minimal degree of water loss during the DMA experiments.

The  $T_\beta$  of the polymeric materials shows the onset of motions of very short segments of polymer chain. The literature on amine-cured DGEBA epoxy have shown that  $T_\beta$  are –61 and –57  $^{\circ}\text{C}$  (at 1 Hz with DMA), and the corresponding activation energies responsible for local-segmental molecular motions are 70 and 67 kJ/mol, respectively [28,29]. The activation energy obtained, based on the frequency dependence of the secondary transition temperature, can be regarded as the energy barrier for molecular motions that are responsible for the creep phenomenon at room temperature. Conversely, large-scale molecular motions are triggered above  $T_g$ . From the linear relationship shown in Fig. 5, it can be proposed that the activation energy remains constant in the range of secondary transition temperature shifts. It can be assumed that the activation energies of the collective molecular motions corresponding to the  $T_\beta$  shift in the linearly viscoelastic region are similar in the temperature ranges starting from arbitrary temperatures below  $T_g$  (e.g., room temperature). Therefore, it is safe to apply the time–temperature superposition principle in this temperature range, due to the linearity in activation energy values.

With regard to the master curve in Figs. 6–8, the linearity between the shift factors in log scale and the reciprocals of testing temperatures in Fig. 9 demonstrates that the time-temperature superposition principle (thermo-rheological simplicity) is applicable to the creep compliance provided the creep deformation remains within the linearly viscoelastic range. Table 4 lists the parameters used in the coupling model for each master curve. The curve-fitting results indicate that the coupling model is capable of describing the creep behavior and estimating the time to reach the equilibrium creep compliance within the linear viscoelastic regime.

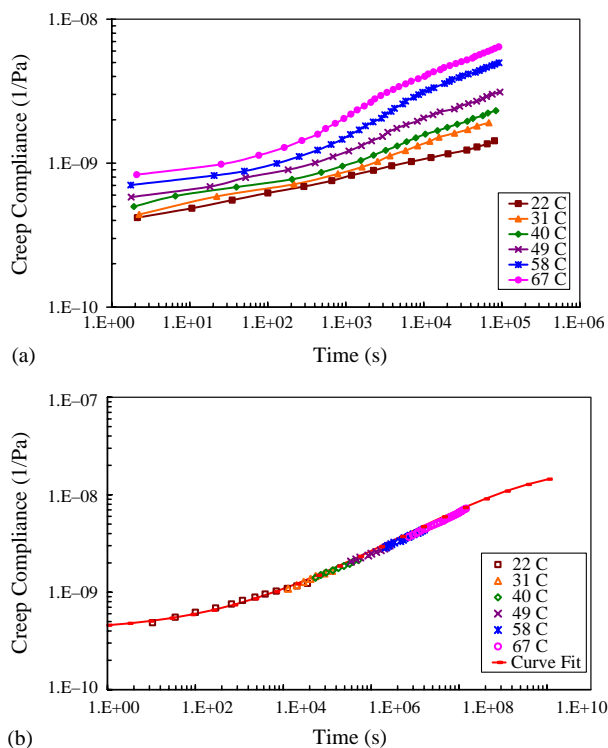


Fig. 6. The creep curves of model systems; (a) individual creep curves and (b) the master curve at 22 °C in the dry condition.

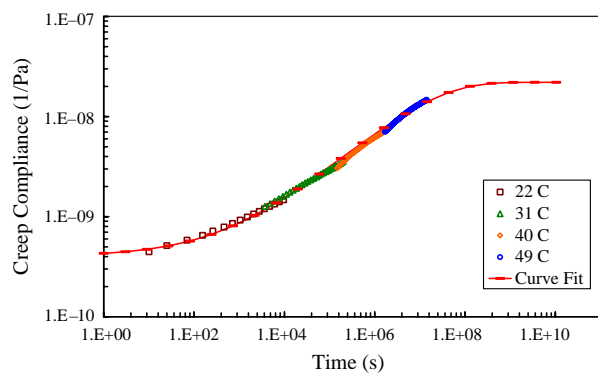


Fig. 7. The master curve of commercial system at 22 °C in the dry condition.

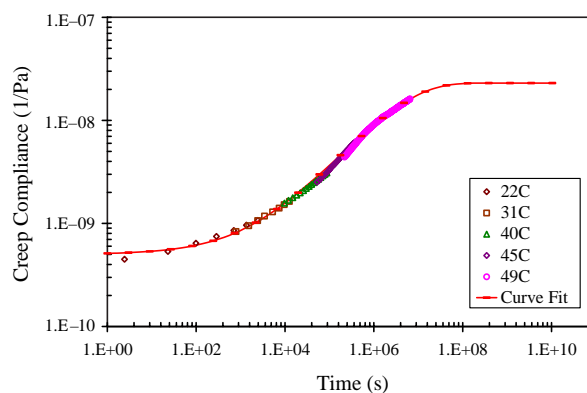


Fig. 8. The master curve of model system at 22 °C in the wet condition.

Young's moduli and rubbery plateau moduli obtained from the tensile (Fig. 2) and DMA tests are both useful for determining the compliance values as time approaches zero and infinity, which allows for the curve fitting to obtain the coupling parameter and apparent relaxation time constants of the epoxy systems. A smaller  $n$  value of the model system in the wet condition suggests that the water in the matrix causes a loosening of molecular constraint. Also, the creep compliance under the wet condition may reach its limit (equilibrium compliance) 1000 times faster than samples under the dry condition. This, in turn, accelerates the creep behavior with the presence of water in the matrix. Similarly, the smaller  $n$  value of the dry commercial epoxy system indicates a weaker creep resistance than the model epoxy system. The presence of additives (flexibilizers and inorganic fillers) in the commercial epoxy system may contribute to this undesirable creep behavior. It is noted that  $n$  and  $T_\beta$  show no direct correlation. This suggests that the scales of molecular motions responsible for  $n$  and  $T_\beta$  are not the same. The scale of molecular motions responsible for the variation in  $n$  is likely to be larger than those responsible for  $T_\beta$  transition. The localized molecular motions responsible for  $T_\beta$  may have helped facilitate larger scale molecular motions upon creep loading to exert creep in epoxy.

It should be pointed out that the creep compliance of the commercial epoxy system, calculated by the rubbery plateau modulus, deviates from the value obtained through curve fitting results of the coupling model results. This discrepancy may be attributed to the presence of the rigid glass-bead fillers in the commercial epoxy system. The fillers can increase the matrix rigidity leading to a higher rubbery plateau modulus of the commercial epoxy system. However, the viscoelastic behavior is generally due to epoxy matrix deformation during the creep tests. This phenomenon may explain why it is not suitable to estimate the equilibrium creep compliance based on the rubbery plateau modulus of the glass bead-filled commercial epoxy system.



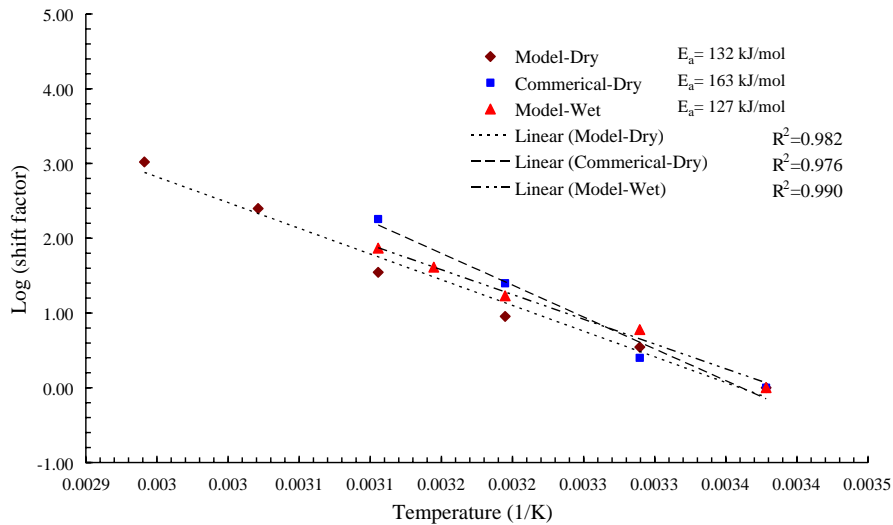


Fig. 9. The Arrhenius relationship between shift factors and temperatures.

Furthermore, the deviation of the creep behavior from the coupling model of the commercial system may be attributable to the non-uniform distribution of the absorbed moisture in epoxy caused by the complex formulation introduced in the commercial system.

It is noted that the activation energies for both the dry and wet samples are very close. This leads to further investigation as to whether there is a simple relationship between the creep responses and absorbed moisture. Epoxy adhesives exhibit a more pronounced creep behavior at elevated temperatures due to a higher molecular mobility. Similarly, the presence of moisture in the epoxy system also accelerates the creep process. It was found that the model epoxy system has a similar viscoelastic response at higher temperatures in a dry condition as samples at lower temperatures in a saturated moisture absorption state (Fig. 10). Fig. 10(a) shows the equivalency between the dry creep compliance at 62°C and the wet creep compliance at 40°C (Case I). Similarly, Fig. 10(b) shows the equivalency between the dry creep compliance at 51°C and the wet compliance at 31°C (Case II). In Table 5, the ratios between the testing temperature and  $T_g$  for the dry and wet conditions were found to be identical for both cases, which implies that an equivalence between temperature and moisture effects on creep behavior may exist in this case.

At 4% absorbed moisture a drop in  $T_g$  corresponding to  $T_{g,wet}/T_{g,dry} = 0.92$  ( $T_g$  expressed in K) for the model system was demonstrated. As for the effect of absorbed moisture on creep behavior, the ratio of the testing temperatures in the dry and wet conditions is 0.93 for Case I and 0.94 for Case II. Interestingly, the ratio of the magnitude of the temperature difference for the viscoelastic creep behaviors is equal to that of the  $T_g$  depression due to the absorbed water in the wet condition. That is, a relationship of the temperature–

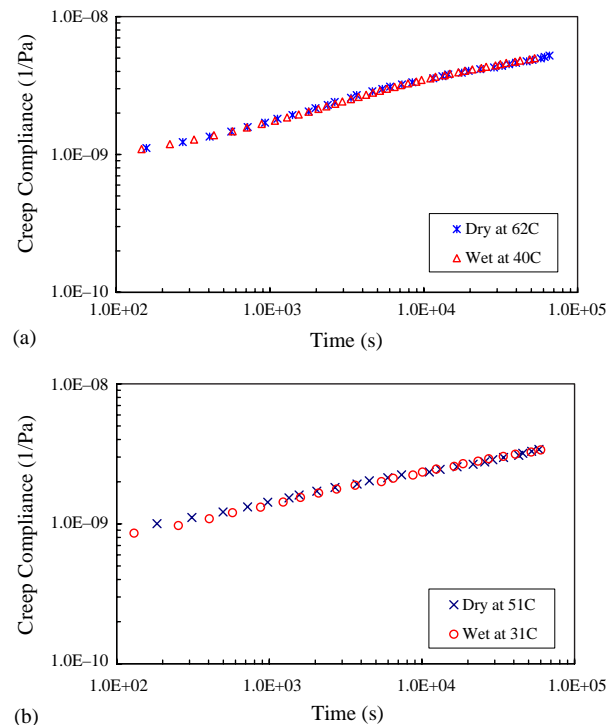


Fig. 10. The equivalence of temperature and moisture effect on creep curves.

moisture equivalence under dry and wet conditions for epoxy can be established by the quantitative analysis in this study.

In summary, the accelerated test method introduced in this paper allows for prediction of the long-term creep behavior of epoxy adhesives. DSC and FTIR techniques were found to be effective in monitoring the possible occurrence of chemical reactions and/or degradation for the fully cured epoxy adhesives during testing. Based on

the moisture diffusion experiments, the moisture absorption at saturation in the humid environment can be reached by means of the accelerated, water immersion tests. This method can also extend the time period of creep tests with a minimal loss of water from the matrix in the wet condition. The time–temperature superposition principle was found to be applicable to both epoxy systems in the linear viscoelastic region. The shift factors as a function of temperature follow the Arrhenius relationship, which allows for construction of a creep compliance master curve in the regions below the  $T_g$ .

Tensile and DMA results can be utilized to estimate the parameters of the coupling model in the linear viscoelastic range. The deviation of the commercial epoxy system from the model prediction was assumed to be due to the complex formulation of this commercial product. The coupling model can be utilized to successfully fit the creep master curves in both dry and wet conditions. The physically based coupling parameter,  $n$ , which corresponds to the constraint of molecular mobility, is useful for describing the state of molecular mobility of epoxy adhesives. Furthermore, the equivalence of temperature and moisture in influencing creep behavior was found to correlate quantitatively in both epoxy adhesive systems.

## 6. Conclusions

A methodology has been established, based on a series of short-term accelerated tests, to study the long-term creep behavior of epoxy adhesives under different environmental conditions. The temperature and moisture effects were also investigated by means of mechanical responses and were found to have equivalent effect on the mechanical responses. The water immersion experiment was found to be a viable method for this set of epoxy adhesives and accelerated the specimens to reach saturation. The time-temperature superposition principle is suitable for constructing a long-term creep master curve for the epoxy adhesives investigated. The physics-based coupling model was found to be effective in describing the long-term creep behavior of epoxy structural adhesives. A reasonable correlation between the temperature and moisture effects on creep behavior was also established. The present findings suggest that the long-term creep behavior of the epoxy structural adhesives can be reliably predicted using a set of short-term accelerated creep tests.

## Acknowledgments

The authors wish to thank J. Huang of Dow Chemical for his guidance for the use of DMA machine and assistance for a portion of DMA tests. The authors also would like to thank Dr. Paul C.K. Chung of the Metal Institute of Research and Development Center for his insightful discussion regarding adhesive testing and durability studies. Special thanks are also given to partial funding from the Metal Institute of Research and Development Center and the Dow Chemical Company.

## References

- [1] Kinloch AJ. Adhesion and adhesives. New York: Chapman & Hall; 1987.
- [2] Ngai KL, White CT. *Physical Rev B* 1979;20:2475.
- [3] Ngai KL, Johscher AK, White CT. *Nature* 1979;277:185.
- [4] Raghavan J, Meshii M. *Composites Sci and Techno* 1997;57:1673.
- [5] Woo EM. *Composites* 1993;25:425.
- [6] Sen A, Bhattacharya M, Stelson KA, Voller VR. *Mater Sci Eng A* 2002;338:60.
- [7] O'Connell PA, McKenna GB. *J Chem Phys* 1999;110:11054.
- [8] O'Brien DJ, Mather PT, White SR. *J Compos Mater* 2001;35:883.
- [9] Crowson RJ, Arridge RGC. *Polymer* 1979;20:737.
- [10] Nielsen LE, Landel RF. *Mechanical properties of polymers and composites*. New York: Marcel Dekker; 1994.
- [11] Al-Haik M, Vaghar M, Garmestani H, Shahaway M. *Composites: Part B* 2001;32:165.
- [12] Ward IM, Hadley DW. *An introduction to the mechanical properties of solid polymers*. New York: Wiley; 1993.
- [13] Pang F, Wang CH. *Composites: Part B* 1999;30:613.
- [14] Li F, Larock RC, Otaigbe JU. *Polymer* 2000;41:4849.
- [15] Kohlrausch R. *Poggendorff Ann Phys Chem J C* 1854;91:179.
- [16] Williams G, Watts DC. *Trans. Faraday Soc.* 1970;66:80.
- [17] Ngai KL, Plazek DJ, Rendell RW. *Rheo Acta* 1997;36:307.
- [18] Ngai KL, Wang Y-N, Magalas LB. *J Alloys and Compounds* 1994;211/212:327.
- [19] Rendell RW, Ngai KL, Fong GR, Yee AF, Bankert RJ. *Polymer Eng Sci* 1987;27:1.
- [20] Plazek DJ, Ngai KL. *Macromolecules* 1991;24:1222.
- [21] Roland CM, Ngai KL, Plazek DJ. *Compos Theor Polym Sci* 1997;7:133.
- [22] Janas VF, McCullough RL. *Compo Sci Techno* 1987;30:99.
- [23] Ferry JD. *Viscoelastic Properties of Polymers*. New York: Wiley; 1980.
- [24] Hunt DG. *Polymer* 1979;20:241.
- [25] Wang JY, Ploehn HJ. *J. Appl Polym Sci* 1996;59:245.
- [26] Crank J, Park GS. *Diffusion in polymers*. London: Academic; 1968.
- [27] Olabisi O, Robeson LM, Shaw MT. *Polymer-polymer miscibility*. New York: Academic Press; 1979.
- [28] Heux L, Halary JL, Laupretre F, Monnerie L. *Polymer* 1997;38:1767.
- [29] Cukierman S, Halary J-L, Monnerie L. *J Non-crystalline Solids* 1991;131:898.